

Tetragonal Nanocrystals from the $\text{Zr}_{0.5}\text{Ce}_{0.5}\text{O}_2$ Solid Solution by Hydrothermal Method

Anwar Ahniyaz, Tomoaki Watanabe, and Masahiro Yoshimura*

Center for Materials Design, Materials and Structures Laboratory, Tokyo Institute of Technology, 4259 Nagatsuta, Midori-ku Yokohama 226-8503, Japan

Received: January 4, 2005; In Final Form: February 11, 2005

The formation of tetragonal $\text{Zr}_{0.5}\text{Ce}_{0.5}\text{O}_2$ solid solution nanocrystallites of 5 ± 1 nm size by a hydrothermal method at 120 °C for 6 h was confirmed by careful Raman and XRD studies for the first time. It was characterized as the t'' -form with an axial ratio of $c/a = 1$ but with oxygen ion displacements. The as-prepared sample was hydrous in nature, which is responsible for the lattice expansion. However, most of the water held in the structure can be expelled by heating the sample above 600 °C. Above 1050 ± 50 °C the t'' -form of tetragonal $\text{Zr}_{0.5}\text{Ce}_{0.5}\text{O}_2$ solid solution dissociates into two phases, cubic phase and the t -form of tetragonal phases.

Introduction

Due to their excellent thermal, mechanical, chemical, electrical, and ionic properties zirconia–ceria solid solutions^{1,2} have attracted much attention for catalysts, sensors, etc. Although their properties strongly depend on the crystal structures, their structural nature is not yet completely understood, particularly for the products prepared at low temperatures, i.e., metastable regions.

The crystal structure of the compositionally homogeneous zirconia-based solid solutions of $\text{Zr}_x\text{Ce}_{1-x}\text{O}_2$ has been studied in detail by Yashima et al. in our laboratory.^{3–8} The existence of three forms of tetragonal phases, all belonging to the $P4_2/nmc$ space group, has been established for the quenched and annealed samples. The stable form of the tetragonal phase is called the t -form, which is restricted in the solubility limit predicted by the equilibrium phase diagram. The t' -form has a wider solubility range, but it is metastable in comparison with the t -form and cubic phase (c -form). Finally, the t'' -form has an axial ratio c/a of unity, but with the oxygen ions displaced from their ideal sites of the cubic phase (8c sites of the $Fm\bar{3}m$ space group) along the c axis.

However, obvious discrepancies and misunderstandings can be found in the literature, because several authors have found problems in distinguishing between the t' and the t'' -forms of tetragonal phases or between the t'' -forms and the cubic phase. Particularly, it is impossible to distinguish between the t'' -form and the cubic form simply by using XRD techniques, because both forms have the same axial ratio ($c/a = 1$), but only the t'' -form has the oxygen displacements.^{3–8} Moreover, the nanocrystallinity of the material makes the problem more complicated due to the XRD line broadening. Thus, Raman and/or neutron diffraction studies must be employed.

Recently, Lamas et al.⁹ reported the existence of the t'' -forms of the tetragonal phase for their nanocrystalline ZrO_2 – CeO_2 samples prepared by the gel-combustion method. Deshpande et al.¹⁰ mentioned the existence of a tetragonal phase in $\text{Zr}_x\text{Ce}_{1-x}\text{O}_2$ ($x > 0.4$) solid solution nanoparticle sols prepared by the sonification of precipitates in an acidic medium. However,

the confirmation of the tetragonal phase for hydrothermally prepared $\text{Zr}_{0.5}\text{Ce}_{0.5}\text{O}_2$ sample has never been reported in detail yet. Since the compositional range of $x = 0.2$ – 0.7 in $\text{Zr}_x\text{Ce}_{1-x}\text{O}_2$ is the two-phase ($t + c$) region at equilibrium in the ZrO_2 – CeO_2 systems, $\text{Zr}_{0.5}\text{Ce}_{0.5}\text{O}_2$ ($x = 0.5$) must be metastably prepared at low temperatures.

Here, we report the confirmation details of the t'' -form of the tetragonal phase formation in the nanocrystalline $\text{Zr}_{0.5}\text{Ce}_{0.5}\text{O}_2 \cdot n\text{H}_2\text{O}$ solid solution prepared by the hydrothermal methods for the first time.

Experimental Section

The $\text{Zr}_{0.5}\text{Ce}_{0.5}\text{O}_2 \cdot n\text{H}_2\text{O}$ sample was produced by hydrothermal treatment of a homogeneous precipitate at 120 °C for 6 h. First, clear solutions of 0.2 M $\text{Ce}(\text{NO}_3)_3$ and $\text{ZrO}(\text{NO}_3)_2$ were made by dissolving $\text{Ce}(\text{NO}_3)_3 \cdot 6\text{H}_2\text{O}$ (99.9%, Nissan Kigenso Co., Ltd) and $\text{ZrO}(\text{NO}_3)_2 \cdot 2\text{H}_2\text{O}$ (Kanto Chemicals) in distilled water. An appropriate amount of mixture solution was then allowed to precipitate using a slight excess amount of NH_4OH (33%, Wako Chemicals) solution with vigorous stirring for a certain period. During the coprecipitation, $\text{pH} \geq 9.0$ was assured and the hydrothermal treatment was carried out in a 50 mL Teflon-lined autoclave, and the products were filtered, washed, and dried at 80 °C for 24 h before being subjected to characterization. An X-ray diffractometer (Model MX 3VA, MAC Science), using $\text{Cu K}\alpha$ radiation ($\lambda = 1.5405$ Å) and operating at 40 mA and 40 kV, was used to obtain the powder diffraction data. An H9000-NAR (Hitachi) was used to take high-resolution TEM photographs of the samples. Thermogravimetric–differential thermoanalysis (TG–DTA) data were traced both for the heating and cooling processes using a thermal analyzer (TG–DTA 2000, Mac Science Co., Ltd). Visible Raman data were collected using a Jobin/Atago Bussan T64000 Triple spectrometer equipped with a 514.5-nm visible laser. Calcination was carried out using a program-controlled furnace (NF50–CB, Nishimura Kogyo Co. Ltd).

Results and Discussion

The XRD pattern of the as-prepared $\text{Zr}_{0.5}\text{Ce}_{0.5}\text{O}_2 \cdot n\text{H}_2\text{O}$ solid solution is shown in Figure 1. It revealed that the as-prepared

* Corresponding author. Tel: 81-45-924-5323. Fax: 81-45-924-5358. E-mail: yoshimura@msl.titech.ac.jp.

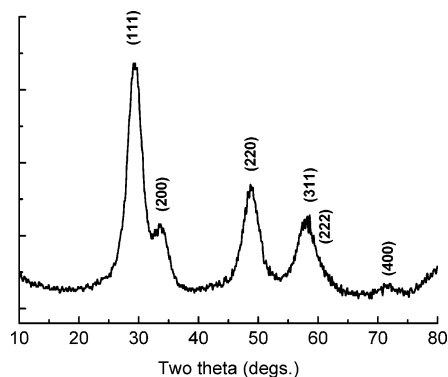


Figure 1. Typical X-ray diffractogram of the Zr_{0.5}Ce_{0.5}O₂·*n*H₂O solid solutions prepared by the hydrothermal method at 120 °C for 6 h.

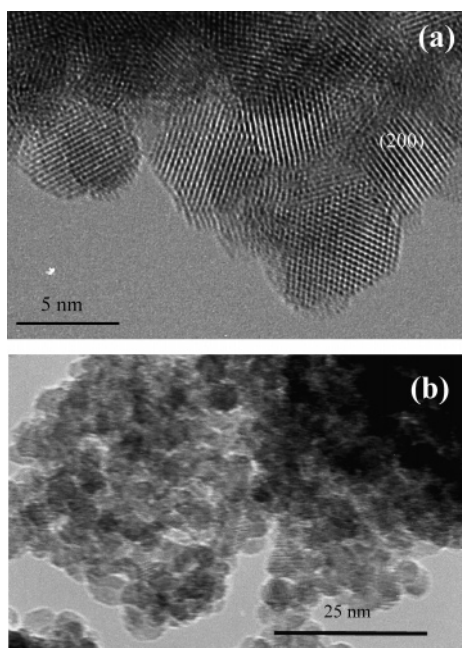


Figure 2. HRTEM micrographs of the Zr_{0.5}Ce_{0.5}O₂·*n*H₂O solid solution prepared at 120 °C for 6 h by the hydrothermal method.

solid solution is nanocrystalline with about a 5 nm size based on the data calculated from Scherrer's equation (Si was used as an internal standard). High-resolution TEM micrographs of the as-prepared sample (Figure 2) also indicated the existence of nanocrystals of about 5 ± 1 nm in size. All the peaks in the XRD pattern of the sample can be indexed by a fluorite-type phase (Figure 1). No clear phase separation can be detected in the present sample, though phase separation has often been observed for Zr_{0.5}Ce_{0.5}O₂ sample prepared at low temperatures.^{11–14} Indeed, the phase separation does happen in general cases due to the different solubility products of both Ce(OH)₃ or Ce(OH)₄ and Zr(OH)₄. However, we have found that such phase separation and segregation can be avoided if the synthesis condition is carefully monitored.¹¹ That is, the complete oxidation of Ce³⁺ to Ce⁴⁺ ions during the coprecipitation process enhances the homogeneous solid solution formation by diminishing the differences in both valency and size between the Zr⁴⁺ and Ce³⁺ cations.¹¹ It seems to indicate that the existence of OH[−] ions in the structure and defect concentration also play an important role in the formation of the fluorite phase at low temperatures for the hydrothermally prepared samples besides the existence of stabilizers¹² and domain boundaries.¹³ Moreover, it is not unreasonable to expect more defects in nanocrystalline samples prepared at low temperature compared to

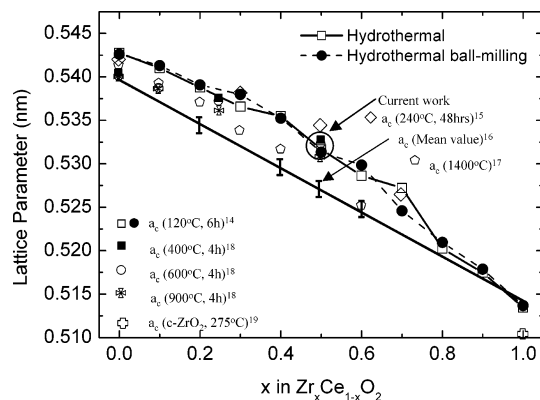


Figure 3. Compositional dependence of the lattice parameters in the Zr_{*x*}Ce_{1−*x*}O₂ solid solution system: (a) ref 14 and this work; (b) ref 15; (c) ref 16; (d) ref 17; (e) ref 18; (f) ref 19.

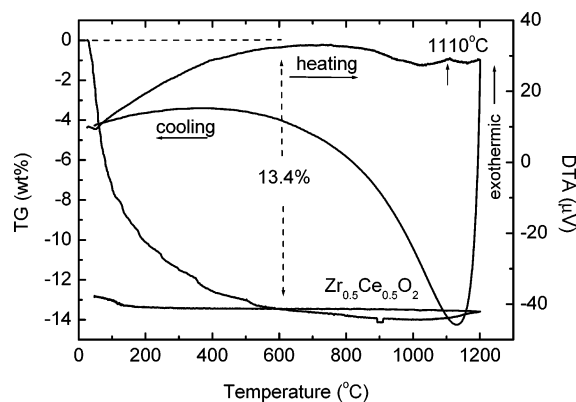


Figure 4. TG–DTA curve of the Zr_{0.5}Ce_{0.5}O₂·*n*H₂O samples prepared by the hydrothermal ball milling at 120 °C for 6 h (10 °C/min).

its bulk counterparts. The defect concentration could have a significant effect on the surface energy. This might be another reason we could get a fluorite-type single-phase solid solution under our experimental conditions.

A serious question exists whether the obtained single phase is really cubic or the *t'*'-form. By only using XRD, we cannot distinguish between them, but we can conclude that it is the *t'*'-form by a Raman analysis that will be described later.

As shown in Figure 3, the calculated lattice parameters of the as-prepared samples by both the hydrothermal method¹¹ and the hydrothermal ball milling method¹⁴ gradually decrease when the zirconia amount increases. By comparison with the data for the samples fired at high temperatures in the zirconia–ceria system, it is found that the hydrothermally prepared samples at low temperatures always tend to have larger lattice parameters. The same phenomenon has also been observed by Hirano et al.¹⁵ for their hydrothermally synthesized samples. However, most previous studies¹⁸ including Hirano's¹⁵ have not mentioned the reason responsible for the lattice expansion in their samples, even though it was so evident in their reports.

We believe that these slight upward shifts in the lattice parameters must be related to the water amount that was held in the fluorite-related structure in these systems. As we expected, the TG–DTA analysis of the Zr_{0.5}Ce_{0.5}O₂·*n*H₂O solid solution sample (Figure 4) showed that the as-prepared sample holds about 13.4 wt % water in its structure, which can be completely expelled by heating the samples above 600 °C for a few hours. This 13.4 wt % water content corresponds to *n* = 1.27 for Zr_{0.5}Ce_{0.5}O₂·*n*H₂O, but it decreases to *n* = 0.52 (about 6 wt %) at 100 °C and then *n* = 0.25 (about 3 wt %) at 200 °C. These results suggest that the majority of water in the as-prepared

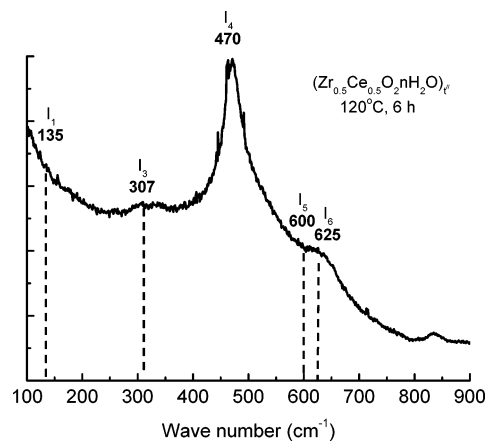


Figure 5. Visible Raman spectra of the as-prepared $\text{Zr}_{0.5}\text{Ce}_{0.5}\text{O}_2 \cdot n\text{H}_2\text{O}$ solid solution at 120 °C for 6 h.

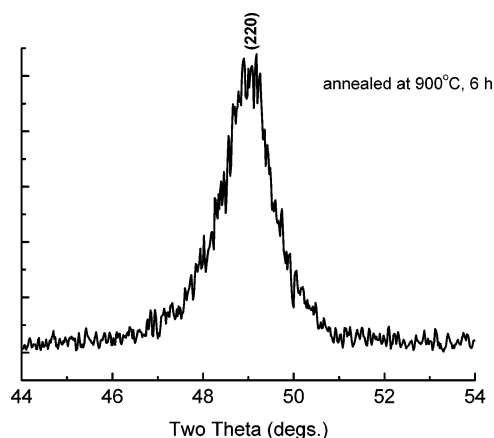


Figure 6. Typical X-ray diffractogram of the annealed sample at 900 °C for 6 h in air.

sample might be surface-absorbed water, but some of the water may exist as OH^- ions in the lattice and could bring about the lattice expansions of the fluorite-related phases. No structural change has been observed in the XRD and Raman spectra from 600 to 1050 ± 50 °C.

To further clarify the structural character of the $\text{Zr}_{0.5}\text{Ce}_{0.5}\text{O}_2 \cdot n\text{H}_2\text{O}$ sample, Raman studies were carried out. As can be clearly seen in the visible Raman spectra (Figure 5), satellites of the tetragonal phase were observed around the characteristic peak of the cubic band, which is located around 470 cm^{-1} . These Raman spectra, which are almost the same as those for the t'' -form in the solid solutions prepared at high temperatures,⁵ indicate that the structure of $\text{Zr}_{0.5}\text{Ce}_{0.5}\text{O}_2 \cdot n\text{H}_2\text{O}$ is not cubic but tetragonal in nature. If it were a cubic lattice, as in the case of CeO_2 , a single peak should appear at 463 cm^{-1} ,²⁰ with peak shifts due to the change in the CeO_2 environment in the presence of ZrO_2 and $\text{ZrO}(\text{OH})_2$ species.^{20,21} In general, a single band corresponding to the F_{2g} for a cubic structure and six bands related to one A_{1g} , three E_g , and two B_{1g} modes for a tetragonal structure are expected.²⁰

As shown in Figure 6, the XRD pattern of the annealed sample at 900 °C for 6 h become sharper, but still can be indexed with a pseudocubic lattice. No apparent peak splitting for a tetragonal lattice has been observed. However, the Raman spectra of the sample (Figure 7) showed clear characteristic peaks of a tetragonal phase. Therefore, the as-prepared $\text{Zr}_{0.5}\text{Ce}_{0.5}\text{O}_2 \cdot n\text{H}_2\text{O}$ sample at 120 °C and the annealed one at 900 °C could be confirmed as the t'' -form of the tetragonal phase having a unit cell with $a/c = 1$ and oxygen displacements in

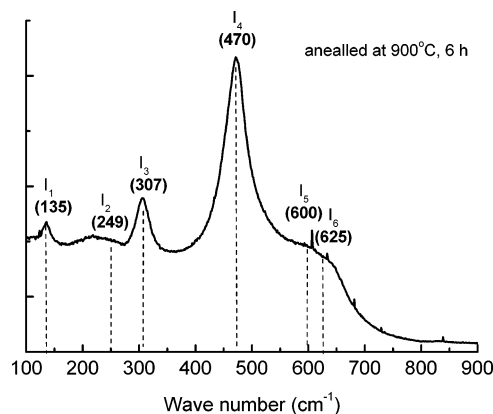


Figure 7. Visible Raman spectra of the annealed $\text{Zr}_{0.5}\text{Ce}_{0.5}\text{O}_2$ solid solution at 900 °C for 6 h.

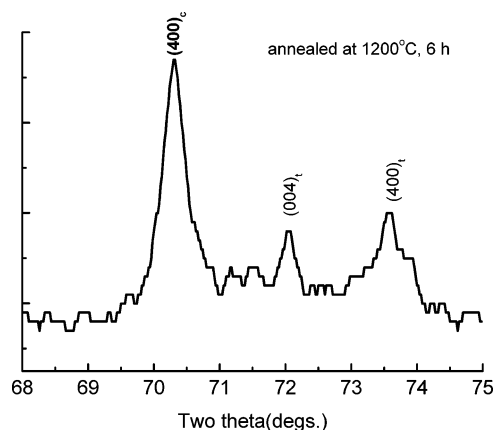


Figure 8. Typical X-ray diffractogram of the annealed sample at 1200 °C for 6 h in air (smoothed).

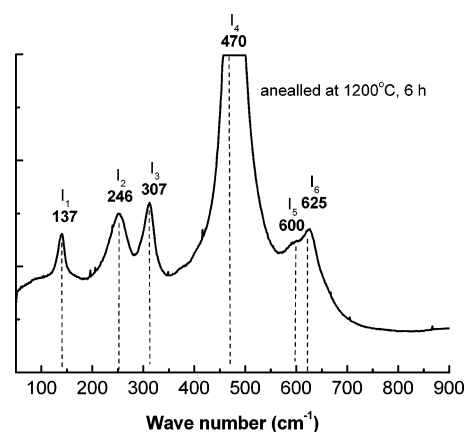


Figure 9. Visible Raman spectra of the annealed $\text{Zr}_{0.5}\text{Ce}_{0.5}\text{O}_2$ solid solution at 1200 °C for 6 h.

the cell. This trend continues until 1050 ± 50 °C, as it can also be observed from Figure 4. A clear exothermic peak around 1100 °C, which was observed in the TG-DTA profile of the sample, is the indication of phase separation. Indeed, both XRD (Figures 8 and 10) and Raman (Figures 9 and 11) analysis results clearly showed the phase separation of this metastable t'' -form of tetragonal phase into two phases, the t -form and the cubic phases at higher temperatures above 1100 °C. As seen in Figures 8 and 10, a single peak—(400) in t'' -form—has changed into three peaks—(400) in a cubic phase and (004) and (400) in a tetragonal phase—by annealing at 1200 or 1400 °C. The compositions calculated from their peak positions of the cubic phase and the tetragonal phases are corresponding to 82% CeO_2

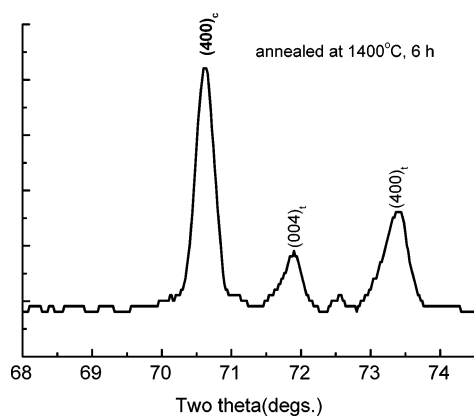


Figure 10. Typical X-ray diffractogram of the annealed sample at 1400 °C for 6 h in air (smoothed).

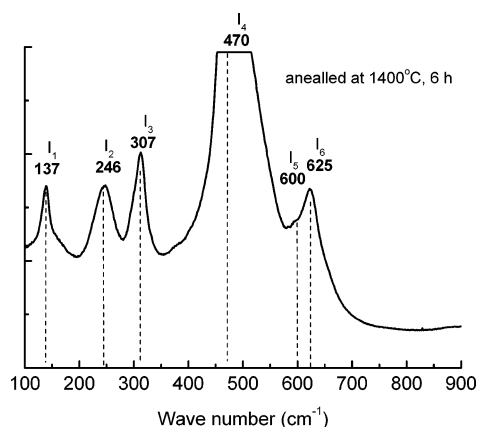


Figure 11. Visible Raman spectra of the annealed Zr_{0.5}Ce_{0.5}O₂ solid solution at 1400 °C for 6 h.

and 12% CeO₂ at 1200 °C and 72% CeO₂ and 16% CeO₂ at 1400 °C. The compositions well-agreed with those of the solubility limits for the cubic solid solution phase and the tetragonal solid solution phase (t-form) at the confirmed equilibrium phase diagram, which was well-established in our group.^{5,17}

Raman data in Figures 9 and 11 also clearly demonstrate that the annealed samples at 1200 and 1400 °C consist of the two phases of cubic and tetragonal phases.

In conclusion, based on both Raman and XRD data for the Zr_{0.5}Ce_{0.5}O₂·*n*H₂O samples prepared at 120 °C, they should be the t''-form⁵ of a metastable tetragonal phase, which has an *a/c* axial ratio of unity but characteristic satellite Raman peaks of the tetragonal phase. This is the first evidence of t''-phase formation at a low temperature. It is in sharp contrast to our previous reports⁵ that the t''-form was formed by annealing the quenched cubic samples with homogeneous compositions at high temperatures. This is another significant point of the current work that provides us with a clue of the possibility of monitoring the t''/t' phase ratio by altering the synthesis processes in the future, as this ratio²² and nanoscale homogeneity²³ are regarded as important indications of the catalytic activity of the material.

Additional problems have widely been claimed as to whether small crystallites with a high surface energy might contribute to the formation of the cubic phase in ZrO₂ and its solid solution.²⁴ This tendency has been observed in almost all studies, but the critical size has never been fixed. It would probably be

a kinetic problem rather than a thermodynamic one. Anyway, the present study revealed that the Zr_{0.5}Ce_{0.5}O₂ particles with a 5 ± 1 nm size crystallized at 120 °C were the tetragonal t''-form.

Conclusion

A careful XRD and Raman study was carried out for the nanocrystalline Zr_{0.5}Ce_{0.5}O₂·*n*H₂O solid solution prepared by the hydrothermal method at 120 °C for 6 h, and it was confirmed as the t''-form tetragonal phase. The as-prepared sample is hydrous in nature and it can be expelled easily by heating above 600 °C without any structural changes until 1050 ± 50 °C. Phase separation of the t''-form into the t-form and the cubic phases occurred at around 1100 °C for the nanocrystalline Zr_{0.5}Ce_{0.5}O₂ solid solution.

Acknowledgment. This project was financially supported by Rhodia, Co. Ltd., Paris, France. We express our appreciation to Drs. H. Catherine, B. Pacaud, L. Dai, P. Macaudiere, C. Magnier, O. Larcher, and E. Rohart of Rhodia for the helpful discussions. The authors express their sincere thanks to Prof. M. Kakihana in our institute for his helpful discussion on Raman studies and Dr. Sakamoto for his help with TEM observation.

References and Notes

- (1) Swartz, S. L. *Catalysis by Ceria and Related Materials* (book review). *J. Am. Chem. Soc.* **2002**, *124*, 12923.
- (2) Rodriguez, J. A.; Hanson, J. C.; Kim, J.-Y.; Liu, G.; Iglesias-Juez, A.; Fernandez-Garcia, M. *J. Phys. Chem. B* **2003**, *107*, 3535.
- (3) Yashima, M.; Morimoto, K.; Ishizawa, N.; Yoshimura, M. *J. Am. Ceram. Soc.* **1993**, *76*, 1745.
- (4) Yashima, M.; Morimoto, K.; Ishizawa, N.; Yoshimura, M. *J. Am. Ceram. Soc.* **1993**, *76* (11), 2865.
- (5) Yashima, M.; Arashi, H.; Kakihana, M.; Yoshimura, M. *J. Am. Ceram. Soc.* **1994**, *77* (4), 1067.
- (6) Yashima, M.; Takashina, H.; Kakihana, M.; Yoshimura, M. *J. Am. Ceram. Soc.* **1994**, *77* (7), 1869.
- (7) Yashima, M.; Kakihana, M.; Yoshimura, M. *Solid State Ionics* **1996**, *86–88*, 1131.
- (8) Yashima, M.; Sasaki, S.; Yamaguchi, Y.; Kakihana, M.; Yoshimura, M.; Mori, T. *Appl. Phys. Lett.* **1998**, *72* (2), 182.
- (9) Lamas, D. G.; Lascalea, G. E.; Juarez, R. E.; Djurado, E.; Perez L.; Walsoe de Reca, N. E. *J. Mater. Chem.* **2003**, *13*, 904.
- (10) Deshpande, A. S.; Pinna, N.; Beato, P.; Antonietti, M.; Niederberger, M. *Chem. Mater.* **2004**, *16*, 2599.
- (11) Ahnizay, A.; Fujiwara, T.; Fujino, T.; Yoshimura, M. *J. Nanosci. Nanotech.* **2004**, *4* (3), 233.
- (12) Tani, E.; Yoshimura, M.; Somiya, S. *J. Am. Ceram. Soc.* **1983**, *66* (1), 11.
- (13) Mistuhashi, T.; Ichihara, M.; Tatsuke, U. *J. Am. Ceram. Soc.* **1974**, *57*, 97.
- (14) Ahnizay, A.; Fujiwara, T.; Fujino, T.; Yoshimura, M. *Solid State Ionics* **2004** (in press).
- (15) Hirano, M.; Miwa, T.; Inagaki, M. *J. Am. Ceram. Soc.* **2001**, *84* (8), 1728.
- (16) Yashima, M.; Ishizawa, N.; Yoshimura, M. *J. Am. Ceram. Soc.* **1992**, *75* (6), 1550.
- (17) Tani, E.; Yoshimura, M.; Somiya, S. *J. Am. Ceram. Soc.* **1983**, *66* (7), 506.
- (18) Escribano, V. S.; Lopez, E. F.; Panizza, M.; Resini, C.; Amores, J. M. G.; Busca, G. *Solid State Sci.* **2003**, *5*, 1369.
- (19) Katz, G. *J. Am. Ceram. Soc.* **1971**, *54* (10), 531.
- (20) Michel, D.; Perez y Jorba, M.; Collongues, R. *J. Raman Spectrosc.* **1976**, *5*, 163.
- (21) Fornasiero, P.; Balducci, C.; Di Monte, R.; Kaspar, J.; Sergio, V.; Gubitosa, G.; Ferrero, A.; Graziani, M. *J. Catal.* **1996**, *164*, 173.
- (22) Si, R.; Zhang, Y.-W.; Li, S.-J.; Lin, B.-X.; Yan, C.-H.; *J. Phys. Chem. B* **2004**, *108*, 12481.
- (23) Mamontov, E.; Brezny, R.; Koranne, M.; Egami, T. *J. Phys. Chem. B* **2003**, *107*, 13007.
- (24) Tsunekawa, S.; Ito, S.; Kawazoe, Y.; Wang, J.-T. *Nano Lett.* **2003**, *3* (4), 871.